DMD Fast Forward. Published on June 24, 2005 as doi:10.1124/dmd.105.005108
This article has not been copyedited and formatted. The final version may differ from this version.

DMD #5108

# UDP-GLUCURONOSYLTRANSFERASE 2B7 IS THE MAJOR ENZYME RESPONSIBLE FOR GEMCABENE GLUCURONIDATION IN HUMAN LIVER MICROSOMES

JONATHAN N. BAUMAN, THEUNIS C. GOOSEN, MEERA TUGNAIT, VINCENT PETERKIN, SUSAN I. HURST, LEE C. MENNING, MARK MILAD, MICHAEL H. COURT AND J. ANDREW WILLIAMS

*Department of Pharmacokinetics, Dynamics and Metabolism, Pfizer Global Research and Development, Ann Arbor, Michigan (J.N.B., T.C.G., M.T., V.P., S.I.H., L.C.M., M.M., J.A.W.) and Department of Pharmacology & Experimental Therapeutics, Tufts University School of Medicine, Boston, MA (M.H.C.)*

**Running Title.** UGT2B7 is the major enzyme catalyzing glucuronidation of Gemcabene

**Corresponding Author:** Jonathan N. Bauman, Department of Pharmacokinetics, Dynamics and Metabolism, Pfizer Global Research and Development, 2800 Plymouth Rd., Ann Arbor, MI 48105. Phone: (734) 622-5603, Fax: (734) 622-4349, Email: jonathan.bauman@pfizer.com

Number of text pages: 22

Number of tables: 2

Number of figures: 6

Number of references: 15

Number of words in Abstract: 247

Number of words in Introduction: 435

Number of words in Discussion: 680

**Abbreviations**: HLM, human liver microsomes; DMSO, dimethyl sulfoxide; HPLC, high-performance liquid chromatography; UDPGA, uridine 5'-diphosphoglucuronic acid; UGT, UDP-glucuronosyltransferase; AZT, zidovudine, 3'-azido-3'-deoxythymidine; HMF, 5, 6, 7, 3', 4', 5'-hexamethoxyflavone; HFC, 7-hydroxy-4-trifluoromethylcoumarin; HPLC-MS, high performance liquid chromatography- mass spectrometry; saccharolactone, D-saccharic acid 1,4-lactone; INN, international nonproprietary name.

DMD Fast Forward. Published on June 24, 2005 as DOI: 10.1124/dmd.105.005108
This article has not been copyedited and formatted. The final version may differ from this version.



## ABSTRACT

The predominant metabolic pathway of gemcabene in humans is glucuronidation. The principal human UDP-glucuronosyltransferases (UGTs) involved in the glucuronidation of gemcabene were determined in this study. Glucuronidation of gemcabene was catalyzed by recombinant UGT1A3, recombinant UGT2B7 and recombinant UGT2B17, as well as by HLM. Gemcabene glucuronidation in recombinant UGTs and HLM followed non-Michaelis-Menten kinetics consistent with homotropic activation, but pharmacokinetics in humans were linear over the dose range tested (total plasma $C_{max}$ 0.06-0.88 mM). Gemcabene showed similar affinity ($S_{50}$) for recombinant UGTs (0.92 -1.45 mM) and HLM (1.37 mM). (S)-Flurbiprofen was identified as a more selective inhibitor of recombinant UGT2B7-catalyzed gemcabene glucuronidation (>23-fold lower $IC_{50}$) when compared with recombinant UGT1A3- or recombinant UGT2B17-catalyzed gemcabene glucuronidation. The $IC_{50}$ for (S)-flurbiprofen inhibition of gemcabene glucuronidation was similar in HLM (60.6 μM) compared with recombinant UGT2B7 (27.4 μM), consistent with a major role for UGT2B7 in gemcabene glucuronidation in HLM. In addition, 5, 6, 7, 3', 4', 5'-hexamethoxyflavone (HMF) inhibited recombinant UGT1A3 and recombinant UGT2B17-catalyzed gemcabene glucuronidation (with 4-fold greater potency for recombinant UGT1A3), but did not inhibit gemcabene glucuronidation in HLM, suggesting that UGT1A3 and UGT2B17 do not contribute significantly to gemcabene glucuronidation. Reaction rates for gemcabene glucuronidation from a human liver bank ($r^2$ = 0.722, P<0.0001, n=24) correlated well with rates of glucuronidation of the UGT2B7 probe substrate 3'-azido-3'-deoxythymidine (AZT). In conclusion, using the three independent experimental approaches

typically utilized for cytochrome P450 reaction phenotyping, UGT2B7 is the major enzyme contributing to gemcabene glucuronidation in human liver microsomes.

## INTRODUCTION

Gemcabene (Figure 1) increases high-density lipoproteins whilst lowering serum triglycerides in humans (Bays and Stein, 2003). Gemcabene is cleared almost exclusively by glucuronidation wth 78% of a radioactive dose recovered in human urine, consisting of 61% glucuronide and 17% unchanged parent drug (Pfizer Global Research and Development, unpublished observations). The primary aim of the present study was to identify the major human UDP-glucuronosyltransferase (UGT) isoform(s) catalyzing the glucuronidation of gemcabene.

To date, at least 17 human UGT's have been identified and twelve are commercially available. Seventeen have been cloned and sequenced, and several of their cDNA's have been heterologously expressed utilizing cell systems to demonstrate substrate specificity (Mackenzie et al., 1997). Similar to cytochrome P450s, individual UGT's have distinct, yet overlapping substrate specificities (Radominska-Pandya et al., 1999) (Tukey and Strassburg, 2000). Historically, phenotyping of drug glucuronidation has received much less attention than cytochrome P450-mediated metabolism, due to a relative lower risk of UGT mediated drug-drug interactions, compared to cytochrome P450s (Williams et al., 2004). The consequent lack of attention to glucuronidation has led to the slower discovery of selective probe substrates and inhibitors useful in the phenotyping of UGT catalyzed reactions (Miners et al., 2004). However, recent advances now make it possible to conduct UGT reaction phenotyping experiments with significantly greater confidence in the resulting data (Court, 2004; Williams et al., 2005). These efforts would help to predict the influence of inter-individual variation in glucuronidation due to

polymorphisms in the encoded proteins, or modulation of protein expression on drug bioavailability, pharmacokinetics, and efficacy.

Definitive cytochrome P450 reaction phenotyping studies typically utilize three approaches to assess the relative contributions of each P450 to the metabolism of the test compound (Bjornsson et al., 2003). These include use of 1) recombinant enzymes, 2) selective chemical inhibition of human liver microsomal metabolism and 3) correlation analyses using a phenotyped human liver bank (Bjornsson et al., 2003). In the case of P450s, relative hepatic expression levels are known. However, the absence of knowledge on the relative expression levels of UGTs in human liver microsomes or recombinantly expressed enzyme systems makes it difficult to quantitatively extrapolate or estimate of the relative contributions of individual UGTs to glucuronidation of the drug in question (Clarke, 1998).

The strategy described in this article to determine the UGT's responsible for gemcabene metabolism is based on the typically used procedures for definitive cytochrome P450 reaction phenotyping (Court, 2004). We were able to identify the major UGT form(s) contributing to gemcabene glucuronidation by 1) characterizing recombinant UGT-catalyzed gemcabene glucuronidation, 2) identifying selective recombinant UGT inhibitors and 3) phenotyping a human liver bank for activities of relevant UGTs.

## Methods

**Chemicals and Reagents.** Unless otherwise indicated, chemicals were purchased from Sigma-Aldrich (St. Louis, MO). Flavones were purchased from Indofine Chemical Company, Inc (Hillsborough, NJ). HPLC-grade methanol and acetonitrile were purchased from Mallinckrodt (Chesterfield, MO). Gemcabene, 6-(5-Carboxy-5-methyl-hexyloxy)-2,2-dimethyl-hexanoic acid (PD0072953), gemcabene-glucuronide, 6-[6-(5-Carboxy-5-methyl-hexyloxy)-2,2-dimethyl-hexanoyloxy]-3,4,5-trihydroxy-tetrahydro-pyran-2-carboxylic acid (PD0329728) and internal standard, 6-(5-Carboxy-5-methyl-heptyloxy)-2-ethyl-2-methyl-hexanoic acid (PD0200455) were all synthesized by the Department of Chemistry, Pfizer Global Research and Development (Ann Arbor, MI), Figure 1.

**Biological Reagents**. Pooled human liver microsomes (mixed gender, *n* = 60), individual liver microsomes from a panel of 24 donors, and recombinant forms of the following UGTs prepared from baculovirus expression systems: UGT1A1, 1A3, 1A4, 1A6, 1A7, 1A8, 1A9, 1A10, 2B4, 2B7, 2B15, and 2B17 (SUPERSOMES™), were purchased from BD Gentest (Woburn, MA).

**Gemcabene Glucuronidation Assay.** Gemcabene was incubated at 37°C with 50 mM Tris-HCl (pH 7.1), 5 mM UDPGA, 5 mM $MgCl_2$, 1 mM saccharolactone (D-glucaric acid-1,4-lactone monohydrate, HLM only), 50 µg alamethicin per mg protein, and pooled HLM (1.25 mg/mL) or recombinant UGT (0.1-0.5 mg/mL) following a 15-minute pre-incubation on ice. The incubation times varied between 15 and 240 minutes. The final incubation volume was 0.2 ml. Reactions were initiated by the addition of UDPGA and were terminated by the addition of 0.1 ml of acetonitrile containing internal standard and placed on ice. For incubations where inhibitors were included, pre-incubation was for 5 minutes at 37°C prior to reaction initiation.

DMD Fast Forward. Published on June 24, 2005 as DOI: 10.1124/dmd.105.005108
This article has not been copyedited and formatted. The final version may differ from this version.



Quenched samples were centrifuged, and the supernatants were analyzed by HPLC-MS. Incubation times and protein concentrations were also established in preliminary studies with both HLMs and expressed UGTs to be within initial linear rate conditions. Glucuronide concentrations were determined using authentic gemcabene glucuronide with a standard curve prepared in complete incubation matrix including UDPGA. Enzyme activities were calculated and expressed as nanomoles per minute per milligram of protein. All experiments were conducted in triplicate and results reported as a mean ± standard deviation.

**Gemcabene Glucuronide Analysis:** HPLC-MS analyses were performed with an Agilent 1100 HPLC system (Agilent, Palo Alto, CA) coupled to an LCQ Advantage mass spectrometer (Finnigan-MAT, San Jose, CA) with a Finnigan atmospheric pressure ionization source operated in the electrospray ionization mode tuned to unit mass resolution. Chromatographic separation was achieved with a C18 column (2.0 x 150 mm, 5 µ, Luna; Phenomenex, Torrance, CA). The mobile phases were 10 mM ammonium acetate (pH 4.5) in water (solution A) and acetonitrile (solution B). The solvent program consisted of an initial isocratic mobile phase mix (15% solution B) for 3 min, followed by a linear gradient from 15 to 80% solution B over 3 min holding for 4 min and returning to initial conditions over 1 min with a flow rate of 0.4 mL/min. The mass spectrometer was operated in the positive ion mode with single ion monitoring for gemcabene glucuronide; m/z 477 and m/z 329 for the internal standard. The capillary was operated at 200°C, the spray voltage was set to 4.5 kV, and nitrogen was employed as a drying gas at a sheath pressure of 20 psi.

**AZT Glucuronidation Assay and Analysis:** Incubation conditions were similar to the gemcabene glucuronidation assay except; AZT (1.5 mM final concentration), HLM (0.25 mg/mL) protein, 30 minute incubation time and the UV response was quantitated by comparison

to a standard curve of AZT-glucuronide using 3-acetamidophenol as the internal standard. Analyses of AZT glucuronide activity were performed on an Agilent Series 1100 platform HPLC system (Agilent Technologies, Palo Alto, CA), using a Phenomenex Aqua, 5μ, C18, 150 x 4.6 mm high performance liquid chromatography column (Phenomenex, Torrance, CA). The mobile phase solution A was 20 mM phosphate buffer (pH 2.2), and solution B was acetonitrile. Initial conditions were 84% A/16% B pumped at 1.0 mL/min. A linear gradient from 16 to 65% B between 0 and 7.1 min was used, followed by 4.9 min re-equilibration at 16% B.

**Estradiol Glucuronidation Assay and analysis :** Incubation conditions were similar to the gemcabene assay except; β-estradiol (25 μM final concentration), HLM (0.50 mg/mL) protein, 30 minute incubation time and the response was quantitated by comparison to a standard curve of estradiol-3-glucuronidation using α-naphthylglucuronide as the internal standard. After 30 min, the reaction was stopped by the addition of 50 μL of formic acid (25% v/v in buffer). Subsequently, 10 μL of α-naphthylglucuronide (internal standard) was added to each sample. The resulting supernatant was analyzed by HPLC-UV. Analysis was performed on a Perkin-Elmer Series 200 autosampler and LC pump equipped with a Perkin Elmer 785A UV/Vis detector and NCI 900 network chromatography interface (Perkin-Elmer, Boston, MA), utilizing an Agilent Zorbax SB-C18, 5μ, 150 x 4.6 mm high performance liquid chromatography column (Agilent, Palo Alto, CA). The mobile phase solution A was 0.1% TFA (trifluoroacetic acid) and solution B was acetonitrile: 0.1% TFA (90:10, %v/v). Initial conditions were 71% A/29% B pumped at 1.0 mL/min. A linear gradient from 29 to 60% B between 0 and 8 min was used, followed by 1 min at 100% B, and then a 4 min re-equilibration at 29% B.

**Enzyme Kinetic Analysis**. Substrate concentration [S] and velocity (v) data were fitted to the appropriate enzyme kinetic model by nonlinear least-squares regression analysis

(Sigmaplot; SPSS, Chicago, IL) (Bjornsson et al., 2003) in order to derive the enzyme kinetic parameters $V_{max}$ (maximal velocity) and $K_m$ (substrate concentration at half-maximal velocity). The Michaelis-Menten model (eq. 1) or the substrate activation models (eq. 2) (Segel, 1975), which incorporates the Hill coefficient ($n$), were used:

$$V = S \times V_{max}/(S + K_m) \quad (1)$$

$$V = S^n (V_{max}/(S^n + S_{50}{}^n) \quad (2)$$

The best fit (to Eq. 1 or Eq. 2) was based on the following criteria, including visual inspection of the data plots (Michaelis-Menten and Eadie-Hofstee), distribution of the residuals, size of the sum of the squared residuals, and the standard deviation of the estimates.

The $IC_{50}$ estimate for the inhibition of gemcabene glucuronidation was determined by nonlinear curve fitting with GraphPad Prizm (GraphPad Software, San Diego, CA).

## Results

**Kinetics of Gemcabene Glucuronidation in Human Liver Microsomes.** Gemcabene glucuronidation best fit a model described by Hill kinetics and the Eadie-Hoftsee plot (Figure 2) indicating homotropic activation. The $S_{50}$ was 1.37 ± 0.12 mM and the *V*max was 6.04 ± 0.38 nmol/min/mg of protein in pooled human liver microsomes (Table 1).

**Gemcabene Glucuronidation by recombinant UGTs.** From the 12 recombinant UGTs (1A1, 1A3, 1A4, 1A6, 1A7, 1A8, 1A9, 1A10, 2B7, 2B15, and 2B17) investigated, three (UGT1A3, UGT2B7, and UGT2B17) demonstrated the ability to catalyze gemcabene glucuronidation (Figure 3). Further experiments were conducted to characterize enzyme kinetics (Table 1, Fig. 4). Similar to the kinetics observed with human liver microsomes, Eadie-Hofstee plots indicated homotropic activation kinetics for gemcabene glucuronidation by UGT1A3, UGT2B7 and UGT2B17, and the observed $S_{50}$ values were similar to those observed for human liver microsomes (Table 1).

**Inhibitors of gemcabene glucuronidation.** Initial screening studies (data not shown) investigated the potential of the following compounds (at 1, 10 and 100 μM concentration) to inhibit HLM-, recombinant UGT1A3-, recombinant UGT2B7- and recombinant UGT2B17-catalyzed gemcabene glucuronidation naproxen, (S)-flurbiprofen, 7', 2', 4'-trimethoxyflavone, 5, 6, 7, 3', 4', 5'-hexamethoxyflavone (HMF), 3, 5, 7, 3', 4'-quercetinpentamethylether, 5, 6, 7-trihydroxyflavone, 6, 4'-dimethoxyflavone, oxazepam, β-estradiol, diclofenac, silibinin, chloramphenicol and hecogenin. These studies suggested that HMF and (S)-flurbiprofen were

DMD Fast Forward. Published on June 24, 2005 as DOI: 10.1124/dmd.105.005108
This article has not been copyedited and formatted. The final version may differ from this version.



selective inhibitors of UGT1A3- and UGT2B7-catalyzed gemcabene glucuronidation, respectively. Subsequent studies were conducted in HLM and in expressed UGT1A3, 2B7 and 2B17 to quantitatively assess the inhibitory potential of (S)-flurbiprofen and HMF to inhibit gemcabene glucuronidation (Fig. 5) and to estimate the relative contributions of individual UGTs to the glucuronidation of gemcabene in human liver microsomes. Substrate (gemcabene) concentrations approximated the $S_{50}$ value for gemcabene glucuronidation catalyzed by HLM (1.4 mM) and by recombinant UGT1A3 (0.92 mM), recombinant UGT2B7 (1.45 mM) and recombinant UGT2B17 (1.37 mM). (S)-Flurbiprofen was more selective at inhibiting recombinant UGT2B7-catalyzed gemcabene glucuronidation ($IC_{50}$ = 27.4 ± 2.9 μM) compared to recombinant UGT1A3 ($IC_{50}$ >1000 μM) and recombinant UGT2B17 ($IC_{50}$ = 653 ± 158 μM) enzymes (Table 2). The $IC_{50}$ for inhibition of gemcabene glucuronidation by recombinant UGT2B7 was similar to that observed for inhibition of HLM glucuronidation ($IC_{50}$ = 60.6 ± 4.9 μM).

**Correlation of gemcabene glucuronidation with AZT and estradiol-3-glucuronidation in HLM.** Rates of gemcabene glucuronidation in microsomes from 24 individual human livers correlated well ($r^2$ = 0.722, $P$ < 0.0001) with rates of glucuronidation of the UGT2B7 probe substrate AZT (Fig. 6a), but not with rates of glucuronidation of β-estradiol (Fig. 6b) ($r^2$ < 0.0001, $P$ = 0.984) at the 3-position, a marker of UGT1A1 activity (Senafi et al., 1994).

DMD Fast Forward. Published on June 24, 2005 as DOI: 10.1124/dmd.105.005108
This article has not been copyedited and formatted. The final version may differ from this version.



**Discussion**

The strategy for this study was to use a combination of experimental methods including HLM and recombinant UGTs to identify and characterize the UGT isoforms involved in gemcabene glucuronidation. To achieve this objective, initial studies were performed with HLM to determine enzyme kinetic parameters and accordingly the appropriate gemcabene concentration ($S_{50}$ = 1.37 mM) for subsequent identification of recombinant UGT activities in a panel of commercially available recombinant UGTs. Since only three recombinant UGTs demonstrated the potential to glucuronidate gemcabene, further experiments focused on attempts to differentiate their relative contributions (comparison of enzyme kinetic parameters between recombinant UGTs and HLM, identification of selective inhibitors, and correlation of probe substrate reaction rates in a human liver bank). In combination, the data presented indicate that UGT2B7 is the primary enzyme contributing to glucuronidation of gemcabene. Since glucuronidation is the major clearance mechanism for the compound, hepatic UGT2B7 appears to be the major determinant of gemcabene elimination in humans.

Characterization of the enzyme kinetic parameters for gemcabene glucuronidation did not differentiate the contribution of recombinant UGT1A3, recombinant UGT2B7 or recombinant UGT2B17 in gemcabene glucuronidation. The observation of homotropic activation kinetics for each recombinant UGT was in agreement with the kinetics observed for gemcabene glucuronidation in HLM. Additionally, $S_{50}$ values were similar for the recombinant UGTs (0.92-1.45 mM) compared with HLM (1.37 mM). The relative hepatic expression levels of UGTs in the liver are unknown, although there is evidence that UGT1A3, UGT2B7 and UGT2B17 (Strassburg et al., 1997) are expressed in the liver. The observation of homotropic activation in

HLM has no apparent influence on gemcabene clearance in humans, which was linear between the total plasma $C_{max}$ of 0.06 and 0.88 mM following multiple dose administration (Pfizer Global Research and Development, unpublished observations). Since exposure increased in a dose-proportional manner up to 0.88 mM (Pfizer Global Research and Development, unpublished observations), the in vivo Km appears to be higher than the highest plasma concentration, which is consistent with the in vitro observations.

Experiments conducted to characterize selective inhibitors of recombinant UGTs identified [S]-flurbiprofen as an effective inhibitor of both recombinant UGT2B7- and HLM-catalyzed gemcabene glucuronidation with similar $IC_{50}$. The lack of inhibitory potency of [S]-flurbiprofen on recombinant UGT1A3- and recombinant UGT2B17-catalyzed gemcabene glucuronidation ($IC_{50}$ > 600 μM) indicates significant potential for UGT2B7 to contribute to gemcabene glucuronidation in HLM. The selective inhibitory effects of HMF on recombinant UGT1A3- but not recombinant UGT2B7-, recombinant UGT2B17-, or HLM-catalyzed gemcabene glucuronidation provide further evidence that UGT2B7 plays a major role in gemcabene glucuronidation.

A human liver bank phenotyped for UGT1A1 and UGT2B7 provided a third approach to assess the relative contributions of these enzymes to the glucuronidation of gemcabene. The observation that gemcabene glucuronidation correlated with UGT2B7 (AZT glucuronidation) reaction rates and not UGT1A1 (estradiol-3-glucuronidation) reaction rates provides further support that UGT2B7 is the major contributor to gemcabene glucuronidation in HLM. The

observation that a correlation was found with the UGT2B7 phenotype, but not with a distinctly different UGT activity, rules out differences in liver quality as the basis for the correlation.

In combination, the selective inhibitor and correlation analysis data suggest that UGT2B7 contributes to approximately 70% of the glucuronidation of gemcabene in HLM. As previously indicated, the magnitude of drug-drug interactions for glucuronidated drugs is typically low (Williams et al., 2004). Based on a high in vitro $K_m$, the potential for similar drug-drug interactions for gemcabene would also be expected to be low. Screening efforts to identify a selective inhibitor also indicated low inhibitory potential for UGT2B7-catalyzed glucuronidation, in comparison to that observed for the most potent inhibitors of cytochrome P450 enzymes, [S]-flurbiprofen demonstrated the lowest in vitro $IC_{50}$, at 24 μM, whereas some cytochrome P450 enzymes have potent (sub-micromolar) $IC_{50}$s (Ekins et al., 2003).

In summary, the combination approach described above, which is typically taken for definitive cytochrome P450 reaction phenotyping, can also be used effectively for UGT reaction phenotyping. Further efforts to characterize selectivity of UGT inhibitors would help optimize this process. The data generated using this approach indicates that UGT2B7 is the major UGT enzyme contributing to glucuronidation of gemcabene in HLM.

**Acknowledgments**

We thank Simon E. Ball for helpful discussions.

## REFERENCES

Bays H and Stein EA (2003) Pharmacotherapy for dyslipidaemia--current therapies and future agents. *Expert Opinion on Pharmacotherapy* **4**:1901-1938.

Bjornsson TD, Callaghan JT, Einolf HJ, Fischer V, Gan L, Grimm S, Kao J, King SP, Miwa G, Ni L, Kumar G, McLeod J, Obach RS, Roberts S, Roe A, Shah A, Snikeris F, Sullivan JT, Tweedie D, Vega JM, Walsh J and Wrighton SA (2003) The conduct of in vitro and in vivo drug-drug interaction studies: a Pharmaceutical Research and Manufacturers of America (PhRMA) perspective. *Drug Metab Dispos* **31**:815-832.

Clarke SE (1998) In vitro assessment of human cytochrome P450. *Xenobiotica* **28**:1167-1202.

Court MH (2004) In vitro identification of UDP-glucuronosyltransferases (UGTs) involved in drug metabolism, in *Optimization in Drug Discovery: In-vitro Methods* (Caldwell ZYaGW ed) pp 185-202, Humana Press, Totowa, New Jersey.

Court MH, Duan SX, von Moltke LL, Greenblatt DJ, Patten CJ, Miners JO and Mackenzie PI (2001) Interindividual variability in acetaminophen glucuronidation by human liver microsomes: identification of relevant acetaminophen UDP-glucuronosyltransferase isoforms. *J Pharmacol Exp Ther* **299**:998-1006.

Ekins S, Stresser DM and Williams JA (2003) In vitro and pharmacophore insights into CYP3A enzymes. *Trends Pharmacol Sci* **24**:161-166.

Mackenzie PI, Owens IS, Burchell B, Bock KW, Bairoch A, Belanger A, Fournel-Gigleux S, Green M, Hum DW, Iyanagi T, Lancet D, Louisot P, Magdalou J, Chowdhury JR, Ritter JK, Schachter H, Tephly TR, Tipton KF and Nebert DW (1997) The UDP glycosyltransferase gene superfamily: recommended nomenclature update based on evolutionary divergence. *Pharmacogenetics* **7**:255-269.

Miners JO, Smith PA, Sorich MJ, McKinnon RA and Mackenzie PI (2004) Predicting human drug glucuronidation parameters: application of in vitro and in silico modeling approaches. *Annu Rev Pharmacol Toxicol* **44**:1-25.

Radominska-Pandya A, Czernik PJ, Little JM, Battaglia E and Mackenzie PI (1999) Structural and functional studies of UDP-glucuronosyltransferases. *Drug Metab Rev* **31**:817-899.

Segel IH (1975) *Enzyme kinetics: Behavior and analysis of rapid equilibrium and steady-state enzyme systems.* Wiley & Sons, New York.

Senafi SB, Clarke DJ and Burchell B (1994) Investigation of the substrate specificity of a cloned expressed human bilirubin UDP-glucuronosyltransferase: UDP-sugar specificity and involvement in steroid and xenobiotic glucuronidation. *Biochem J* **303 ( Pt 1)**:233-240.

Strassburg CP, Oldhafer K, Manns MP and Tukey RH (1997) Differential expression of the UGT1A locus in human liver, biliary, and gastric tissue: identification of UGT1A7 and UGT1A10 transcripts in extrahepatic tissue. *Mol Pharmacol* **52**:212-220.

Tukey RH and Strassburg CP (2000) Human UDP-glucuronosyltransferases: metabolism, expression, and disease. *Annu Rev Pharmacol Toxicol* **40**:581-616.

Williams JA, Bauman JN, Cai H, Conlon K, Hansel S, Hurst S, Sadagopan N, Tugnait M, Zhang L and Sahi J (2005) In vitro ADME phenotyping in drug discovery: Current challenges and future solutions. *Current Opinion in Drug Discovery & Development* **8**:78-88.

Williams JA, Hyland R, Jones BC, Smith DA, Hurst S, Goosen TC, Peterkin V, Koup JR and Ball SE (2004) Drug-drug interactions for UDP-glucuronosyltransferase substrates: a pharmacokinetic explanation for typically observed low exposure (AUCi/AUC) ratios. *Drug Metab Dispos* **32**:1201-1208.

DMD Fast Forward. Published on June 24, 2005 as DOI: 10.1124/dmd.105.005108
This article has not been copyedited and formatted. The final version may differ from this version.



**Legends for Figures**

**Figure 1. Chemical structures of gemcabene, gemcabene glucuronide, internal standard, S-flurbiprofen and HMF.**

**Figure 2. Velocity versus substrate concentration (left panel) and Eadie-Hofstee plot (right panel) of the kinetics of gemcabene glucuronidation in pooled human liver microsomes.**

The left panel shows a sigmoidal curve, whereas the right panel shows the curved plot diagnostic of homotropic activation kinetics. This observation appears to have no in vivo relevance, as gemcabene was shown to demonstrate linear pharmacokinetics in humans.

**Figure 3. Gemcabene is glucuronidated by recombinant UGT1A3, UGT2B7 and UGT2B17.**

Glucuronidation was measured at 1.37 mM (triplicate data from two experiments).

**Figure 4. Enzyme kinetics for UGT1A3- (●, left panel), UGT2B7- (▲, middle panel), and UBT2B17- (■, right panel) catalyzed gemcabene glucuronidation.**

Top panels show velocity versus substrate concentration. Bottom panels show Eadie Hofstee plots diagnostic of homotropic activation.

DMD Fast Forward. Published on June 24, 2005 as DOI: 10.1124/dmd.105.005108
This article has not been copyedited and formatted. The final version may differ from this version.



**Figure 5. Inhibition of HLM- (▲), recombinant UGT1A3- (●), recombinant UGT2B7- (▲), or recombinant UGT2B17- (■) catalyzed gemcabene glucuronidation by (S)-flurbiprofen (left panel) or HMF (right panel).**

The data presented in the semi-logarithmic plots indicate that (S)-flurbiprofen has similar potency ($IC_{50}$<70μM) towards inhibition of recombinant UGT2B7 or HLM, and is less potent ($IC_{50}$>600μM) towards UGT1A3 or UGT2B17. Additionally, HMF has much greater inhibitory potency ($IC_{50}$<30 μM) towards UGT1A3 compared to recombinant UGT2B7, recombinant UGT2B17 or HLM ($IC_{50}$ >100μM) in each case.

**Figure 6. Correlation between CI-1027 glucuronidation ($S_{50}$ concentration, 1.37 mM) and UGT2B7-catalyzed AZT glucuronidation (left panel) or UGT1A1-catalyzed estradiol-3-glucuronidation samples from a human liver bank (n=24).**

**Tables**

**Table 1. Kinetic parameters, for gemcabene glucuronidation in human liver microsomes and recombinant UGT1A3, recombinant UGT2B7, and recombinant UGT2B17.**

| Matrix | $S_{50}$[a] | $V_{max}$[a] | Hill Coefficient[a] (*n*) |
|---|---|---|---|
| | mM | nmol/mg/min | |
| HLM | 1.37 ± 0.12 | 6.04 ± 0.38 | 1.8 ± 0.2 |
| UGT1A3 | 0.92 ± 0.06 | 0.38 ± 0.02 | 2.4 ± 0.3 |
| UGT2B7 | 1.45 ± 0.39 | 1.44 ± 0.27 | 1.6 ± 0.3 |
| UGT2B17 | 1.37 ± 0.10 | 0.13 ± 0.01 | 2.4 ± 0.3 |

[a]Mean ± standard deviation of three experiments. HLM and recombinant UGTs were pretreated with alamethacin (50 μg/mg protein) and incubated with varying concentrations of gemcabene in order to determine kinetic parameters as described under Materials and Methods. The data were fitted to the Hill equation ($S_{50}$).

**Table 2. Inhibition of gemcabene glucuronidation in human liver microsomes and recombinant UGTs with (S)-flurbiprofen and HMF.**

| Matrix | $IC_{50}$[a] | |
|---|---|---|
| | (S)-Flurbiprofen | HMF |
| | μM | μM |
| HLM | 60.6 ± 4.9 | >300 |
| UGT1A3 | >1000 | 24.3 ± 1.2 |
| UGT2B7 | 27.4 ± 2.9 | >300 |
| UGT2B17 | 653 ± 158 | 95.4 ± 11.5 |

[a]Mean ± standard deviation of three experiments. $IC_{50}$s for the inhibition of gemcabene glucuronidation by (S)-flurbiprofen and HMF were determined using substrate concentrations approximating the $S_{50}$ values determined in HLM (1.37 mM) and each recombinant UGT isozyme (1A3 - 0.92, 2B7 - 1.45 and 2B17 - 1.37 mM).

Figure 1

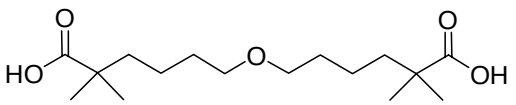


Gemcabene

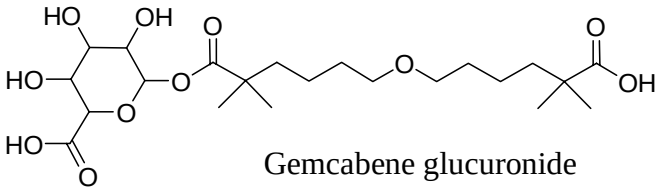


Gemcabene glucuronide

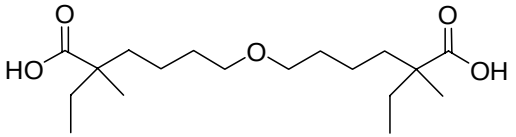


Internal Standard (PD0200455)

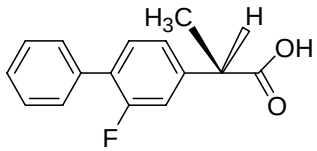


(S)-Flurbiprofen

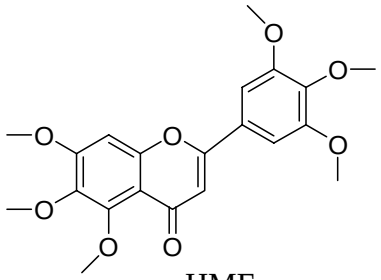


HMF

DMD Fast Forward. Published on June 24, 2005 as DOI: 10.1124/dmd.105.005108
This article has not been copyedited and formatted. The final version may differ from this version.

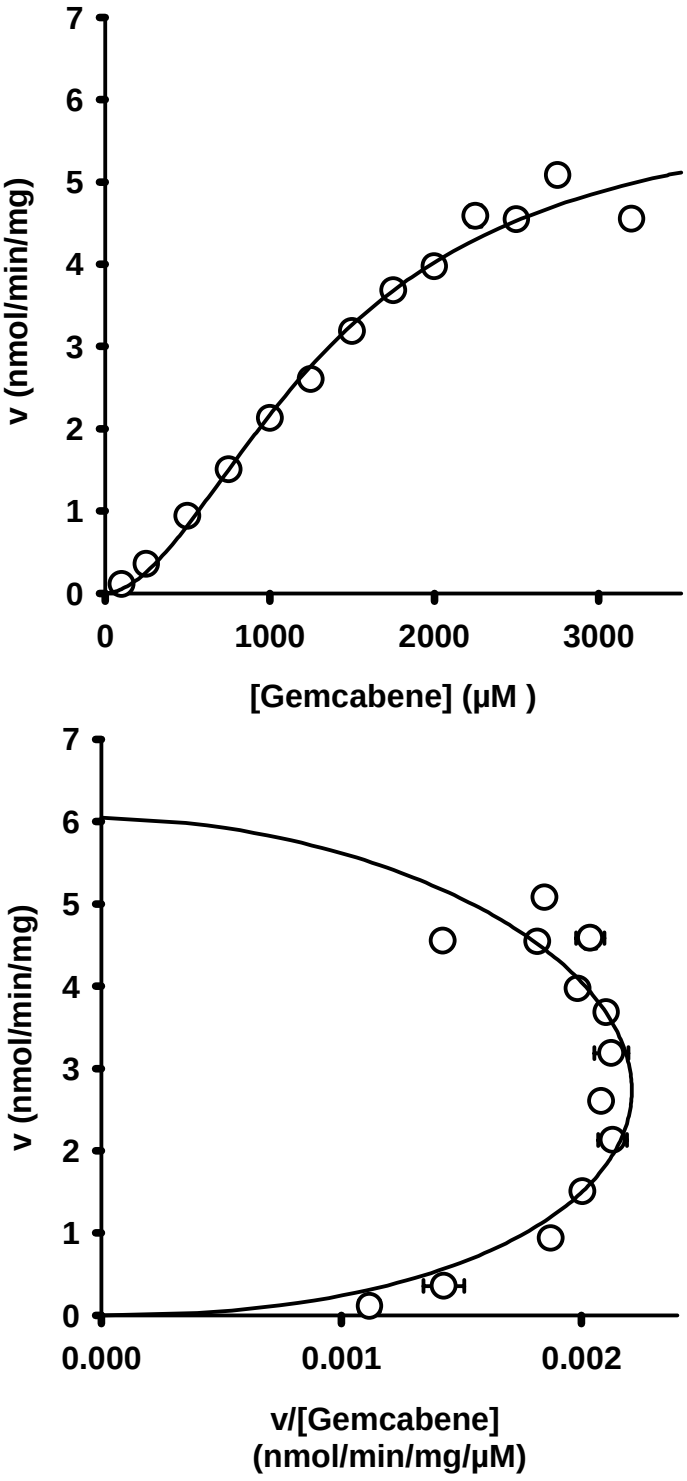


Figure 2

DMD Fast Forward. Published on June 24, 2005 as DOI: 10.1124/dmd.105.005108
This article has not been copyedited and formatted. The final version may differ from this version.

Figure 3

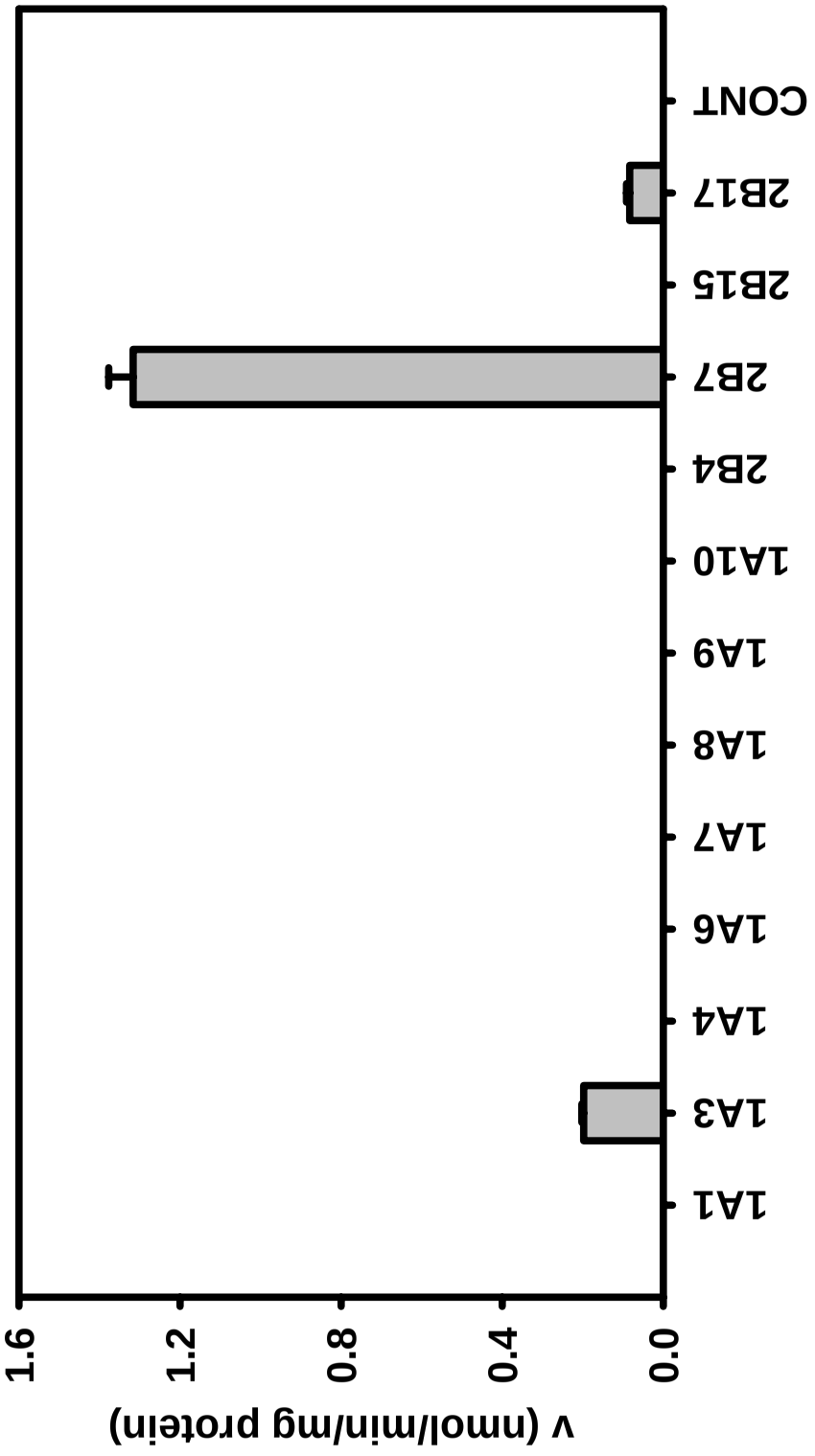

DMD Fast Forward. Published on June 24, 2005 as DOI: 10.1124/dmd.105.005108
This article has not been copyedited and formatted. The final version may differ from this version.

# Figure 4

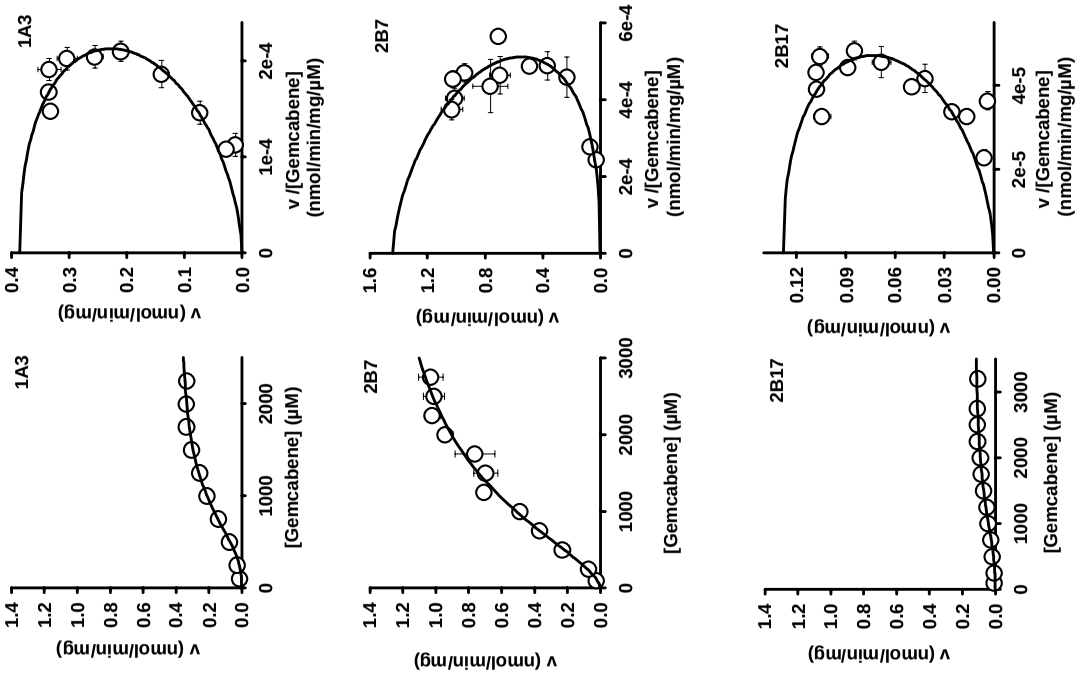

# Figure 5

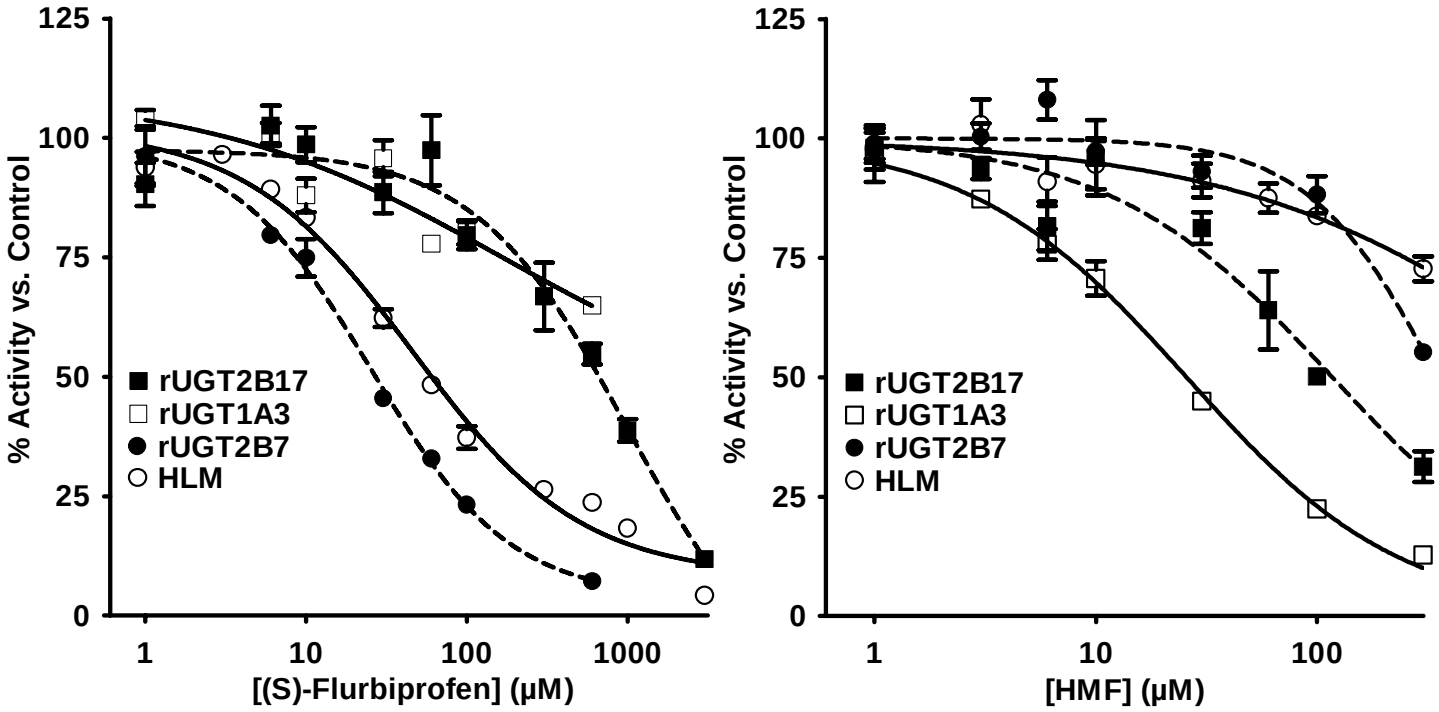

DMD Fast Forward. Published on June 24, 2005 as DOI: 10.1124/dmd.105.005108
This article has not been copyedited and formatted. The final version may differ from this version.

# Figure 6